JOURNAL OF PROPULSION AND POWER
Vol. 18, No. 5, September–October 2002

Effects of Halons and Halon Replacements on Hydrogen-Fueled Laminar Premixed Flames

C. H. Kim,* O. C. Kwon,† and G. M. Faeth‡
University of Michigan, Ann Arbor, Michigan 48109-2140

Fundamental unstretched laminar burning velocities and flame response to stretch, as characterized by Markstein numbers, were considered experimentally and computationally. The investigation was limited to laminar premixed flames involving hydrogen burning in air with Halon 1301 (CF_3Br), nitrogen, and carbon dioxide considered as flame suppressing diluents. Outwardly propagating spherical laminar premixed flames were observed for fuel equivalence ratios of 0.6–1.8, concentrations of oxygen in oxygen/nitrogen mixtures of 21% by volume before dilution with a suppressant, and normal temperature and pressure. Suppressants involved concentrations of the chemically active suppressant, Halon 1301, of 0–2% by volume and concentrations of the chemically passive (chemically inert) suppressants, nitrogen and carbon dioxide, of 0–50% by volume. The present flames were sensitive to flame stretch, yielding values of unstretched-to-stretched laminar burning velocities in the range of 0.6–1.2 for levels of flame stretch well below quenching conditions, for example, for Karlovitz numbers less than 0.15. The agreement between measured and predicted unstretched laminar burning velocities was good based on the mechanisms of Mueller et al. for H_2/O_2 reactions and Babushok et al. for halogen reactions. The resulting flame structure predictions suggest that H and OH radical production and transport are important for flame suppression and preferential-diffusion/stretch interactions; this reflects the strong correlation between laminar burning velocities and the maximum concentrations of H and OH in the reaction zone of the present flames. It also was found that effects of flame suppression that reduced concentrations of H and OH in the reaction zone made the present flames more unstable to preferential-diffusion/stretch interactions, an effect that tends to counteract the beneficial effects of flame suppressants to some extent.

Nomenclature

D	=	mass diffusivity
K	=	flame stretch, Eq. (1)
Ka	=	Karlovitz number, KD_u/S_L^2
L	=	Markstein length
Ma	=	Markstein number, L/δ_D
P	=	pressure
r_f	=	flame radius
S_L	=	laminar burning velocity based on unburned gas properties
S_L'	=	value of S_L at the largest radius observed
T	=	temperature
t	=	time
X_i	=	mole fraction of species i
δ_D	=	characteristic flame thickness, D_u/S_L
ρ	=	density
ϕ	=	fuel-equivalence ratio

Subscripts

b	=	burned gas
max	=	maximum observed value
supp	=	suppressant property
u	=	unburned gas
∞	=	unstretched flame condition

Received 8 August 2001; revision received 29 March 2002; accepted for publication 30 April 2002.

*Graduate Student Research Assistant, Department of Aerospace Engineering.

†Research Fellow, Department of Aerospace Engineering; currently Research Associate, Department of Aerospace and Mechanical Engineering, University of Southern California, Los Angeles, CA 90089.

‡Professor, Department of Aerospace Engineering; gmfaeth@umich.edu. Fellow AIAA.

Introduction

EVEN relatively early studies of premixed flames showed that flame/stretch interactions due to effects of preferential diffusion of various species and heat can significantly affect the laminar burning velocities and structure of laminar premixed flames[1–6] and can also affect the propagation velocities of turbulent premixed flames typical of practical applications.[7,8] Motivated by these observations, several studies of the flame/stretch interactions of laminar premixed flames involving hydrogen, wet carbon monoxide, and hydrocarbons as fuels, with oxidation by both air and various oxygen/diluent mixtures, were completed in this laboratory.[9–16] A finding of these studies is that flame structure predictions suggested that H- and OH-radical production and transport are important aspects of preferential-diffusion/stretch interactions.[16] This is not surprising, however, due to the well-known correlation between laminar burning velocities and H-radical concentrations in hydrogen-fueled laminar premixed flames pointed out by Padley and Sugden[17] based on the laminar burning velocity measurements of Jahn as cited in Ref. 18. Another aspect of these findings is that changes of flame conditions that tended to reduce the concentrations of the H radical in the reaction zone also tended to make these flames more unstable to preferential-diffusion instability. This has the potential to increase flame propagation velocities due to the creation of flame surface area by the distortion or wrinkling of the flame surface as a result of the action of preferential-diffusion instability. On the other hand, it is widely recognized that the action of flame suppressants is mainly governed by their capabilities to reduce H-radical concentrations in the reaction zone,[19–24] which also is in agreement with the findings of Padley and Sugden.[17] Thus, the application of flame suppressants involves an interesting dichotomy: Suppressants have the capability to reduce H-radical concentrations in the reaction zone, which leads to corresponding reductions of laminar burning velocities and tends to reduce fire risk, whereas the same capability of suppressants to reduce H-radical concentrations

in the reaction zone also enhances the potential for development of preferential-diffusion induced flame surface instabilities and, thus, increased flame propagation velocities and tends to increase fire risk.

Motivated by these observations, the objectives of the present investigation were to consider effects of flame suppressants on both unstretched laminar burning velocities and flame response to stretch characterized by Markstein[2] numbers. Experimental and computational methods were used to study premixed laminar flames involving mixtures of hydrogen and air along with Halon 1301 (CF_3Br), a typical chemically active type of flame suppressant, and nitrogen and carbon dioxide, typical of chemically passive (chemically inert) or thermal-quenching types of flame suppressants. Reactant mixtures were limited to normal temperature and pressure (NTP), for example, room temperature and atmospheric pressure. Both measurements and predictions considered outwardly propagating spherical laminar premixed flames, similar to past work in this laboratory[8–16] because observations of these flames readily yield both unstretched laminar burning velocities and Markstein numbers.

Experimental Methods

Apparatus

Experimental methods were similar to past work and will be described very briefly; see Refs. 8–16 for more details. The experiments were conducted in a spherical windowed chamber having an inside diameter of 360 mm. The reactant mixture was prepared in the chamber by adding gases at appropriate partial pressures to reach the specified test pressure, 1 atm for the results presented here. The reactant gases were mixed using a small metal fan located within the chamber with the fan-induced motion allowed to decay before ignition (10 min for mixing and 20 min for decay). The combustible mixture was spark ignited at the center of the chamber using minimum spark ignition energies to minimize ignition disturbances. The flames were observed using high-speed (4000–7500 pictures per second) motion picture shadowgraphy. Once combustion was complete, the chamber was vented and then flushed with air to remove condensed water vapor and to cool it to the allowable initial temperature range of the experiments (298 ± 3 K).

Data Reduction

Present measurements were limited to flames having diameters larger than 10 mm, to avoid ignition disturbances, and smaller than 60 mm, to limit pressure increases during the measuring period to values smaller than 0.7% of the initial pressure. No results were considered where the flame surface was distorted or wrinkled due to effects of buoyancy or flame instability. Similar to earlier work,[8–16] determinations of Markstein numbers were limited to $\delta_D/r_f < 2\%$ so that effects of curvature and transient phenomena associated with large flame thicknesses were negligible. Finally, radiative heat losses were small due to the relatively large laminar flame speeds of hydrogen-fueled flames and were ignored similar to past work.[8–16] For such conditions, the laminar burning velocity and flame stretch are given as follows[3]:

$$S_L = \left(\frac{\rho_b}{\rho_u}\right)\frac{\mathrm{d}r_f}{\mathrm{d}t}, \qquad K = \left(\frac{2}{r_f}\right)\frac{\mathrm{d}r_f}{\mathrm{d}t} \tag{1}$$

The density ratio appearing in Eq. (1) was found from McBride et al.[25] and Reynolds,[26] both yielding the same results, assuming adiabatic constant-pressure combustion with chemical equilibrium in the combustion product gases and the same element concentrations in both the unburned and burned gases. This is a convention that follows past practice,[8–16] however, because it ignores preferential-diffusion effects that modify local element mass fractions and energy transport and causes ρ_b/ρ_u to differ from plane adiabatic flame conditions. This convention is convenient, however, because a single density ratio relates all flame speeds at a given reactant mixture condition. In addition, the convention retrieves the correct flame displacement velocity, $\mathrm{d}r_f/\mathrm{d}t$, for given unburned mixture conditions and degree of flame stretch. Based on past numerical simulations of stretched hydrogen-fueled flames, however, the assumptions used to find ρ_b/ρ_u are quite reasonable for the experimental results reported here, for example, for $\delta_D/r_f < 2\%$, because values of ρ_b/ρ_u for stretched flames agree with those for unstretched (plane) flames within 10% (Ref. 27).

Final results were obtained by averaging the measurements of 4–6 tests at each condition. The resulting experimental uncertainties (95% confidence) are as follows: S_L less than 10%, Karlovitz number less than 20%, and $|Ma|$ less than 25% for $|Ma| > 1$ and less than $25/|Ma|$% for $|Ma| < 1$.

Data Correlation

The measurements were analyzed to find flame/stretch interactions (Markstein numbers) similar to past studies in the literature.[8–16] Considerations were limited to the thin flame limit ($\delta_D/r_f < 2\%$) for conditions where effects of ignition disturbances and flame radiation were small, as mentioned earlier. Then, a convenient relationship between the laminar burning velocity and flame stretch can be obtained by combining an early proposal of Markstein and the local conditions hypothesis of Kwon et al.[8] to yield

$$S_{L\infty}/S_L = 1 + MaKa \tag{2}$$

where values of S_L and Karlovitz number Ka, the dimensionless flame stretch ($= K\delta_D/S_L$), were found from Eqs. (1) as already discussed. For these definitions, δ_D is based on the stretched laminar burning velocity and mass diffusivity of the fuel in the unburned gas, as conventions. The small stretch limit is also of interest to connect present results at finite levels of stretch to the conditions of classical asymptotic theories of laminar premixed flame propagation, at negligibly small levels of stretch, as follows[10]:

$$S_L/S_{L\infty} = 1 - Ma_\infty Ka_\infty, \qquad |Ka_\infty| \ll 1 \tag{3}$$

Several other proposals have been made to represent effects of flame stretch on laminar burning velocities[28–32]; nevertheless, Eq. (2) is particularly convenient because Markstein number Ma has proven to be relatively constant for particular reactant mixture conditions over wide ranges of Karlovitz number Ka, based on both measurements and detailed numerical simulations of laminar premixed flames.[8–16] Thus, $S_{L\infty}$ and Markstein number Ma provide convenient and concise measures of laminar premixed flame burning rates and response to stretch, as discussed by Aung et al.[10] As a result, this approach will be used to summarize the findings of the present investigation. Other advantages of the present characterization of premixed-flame/stretch interactions can be summarized as follows[11]: Data reduction is direct and does not involve the use of flame structure models that are difficult to define and are likely to be revised in the future; the characterization is concise, which facilitates its use by others; the positive and negative ranges of Markstein number provide a direct indication of stable and unstable flame surface conditions with respect to effects of preferential diffusion; and the results can be readily transformed to provide direct comparisons with other ways to characterize preferential-diffusion/stretch interactions. Note, however, that the present approach has only been applied to outwardly propagating spherical laminar premixed flames when $\delta_D/r_f < 2\%$ and effects of ignition disturbances and radiation are small; therefore, use of the present values of Markstein number to characterize effects of flame stretch on laminar burning velocities for other circumstances should be approached with caution.

Test Conditions

Experimental conditions are summarized in Table 1: They involved reactant mixtures at normal temperatures (298 ± 3 K) and atmospheric pressure for hydrogen burning in air at fuel-equivalence ratios of 0.6–1.8. The values of ρ_u/ρ_b and T_b in Table 1 were found from McBride et al.[25] and Reynolds,[26] as discussed earlier. In addition to hydrogen/air flames with no flame suppressants, effects of suppressants on flame properties were measured with the reactant mixture diluted with Halon 1301, nitrogen, or carbon dioxide. Maximum concentrations of the suppressant in the reactant mixture

Table 1 Summary of H_2/air/suppressant flame test conditions[a]

X_{supp}	ϕ	ρ_u/ρ_b	T_o, K	$S_{L\infty}$, mm/s	Ka_{max}	Ma
			No suppressant			
0	0.6	5.55	1840	890	0.10	−1.7
0	1.0	6.89	2380	2070	0.09	0.0
0	1.8	6.30	2130	2920	0.05	2.4
			With Halon 1301			
0.005	0.6	5.60	1830	620	0.39	−1.9
0.005	1.0	6.94	2370	1760	0.09	−0.8
0.005	1.8	6.34	2120	2450	0.06	1.7
0.010	0.6	5.65	1820	460	0.49	−2.2
0.010	1.0	6.99	2350	1280	0.16	−1.1
0.010	1.8	6.38	2110	2070	0.07	1.5
0.020	0.6	5.75	1810	180	0.75	−2.4
0.020	1.0	7.09	2330	950	0.16	−2.2
0.020	1.8	6.46	2080	1400	0.10	1.4
			With nitrogen			
0.010	0.6	5.51	1820	820	0.20	−1.7
0.010	1.0	6.86	2370	2070	0.04	−0.4
0.010	1.8	6.26	2120	2870	0.05	2.5
0.020	0.6	5.48	1810	770	0.25	−1.7
0.020	1.0	6.83	2360	1980	0.08	−1.0
0.020	1.8	6.22	2100	2760	0.05	2.2

[a]Reactants at 298 ± 3 K and 1 atm, $D_u = 72.9$ mm^2/s.

(percent by volume) were as follows: Halon 1301, 2% and nitrogen and carbon dioxide, 50%. The measurements involved Karlovitz numbers of 0–0.75, ratios of unstretched-to-stretched laminar burning velocities of 0.6–1.2, and values of unstretched laminar burning velocities of 180–2920 mm/s.

Computational Methods

Numerical Simulations

Numerical simulations were limited to unstretched (plane) flames and were carried out using the PREMIX code of Kee et al.[33] with thermochemical and transport data obtained from Kee et al.[34,35] An exception was the transport properties of HO_2, which were obtained from Kim et al.[36] Before computing flame properties, all thermochemical and transport properties based on the results of Refs. 34–36 were checked against original sources. Effects of radiation were small due to the generally large flame speeds of hydrogen-fueled flames and were ignored. Calculations carried out for various computational grids, etc., suggest that the numerical errors for predictions of global flame properties (S_L, δ_D, maximum radical concentrations, etc.) were smaller than 2%.

Chemical Reaction Mechanism

The chemical kinetic mechanism and reaction parameters for H/O reactions were obtained from Mueller et al.[37] based on the good performance of this approach for both unstretched and stretched laminar premixed flames involving H/O combustion reported by Kwon and Faeth.[16] The effect of Halon 1301 on flame properties was treated using the bromine reaction mechanism and reaction parameters of Babushok et al.[21] The concentrations of Halon 1301 in the present flames were smaller than 2 vol%, however, so that effects of reactions of CF_3, which enters the flames as a component of Halon 1301, were small and were ignored. Reactions of nitrogen and carbon dioxide were also ignored, that is, they were treated as passive diluents. Thus, the final $H_2/O_2/CF_3Br/N_2$ mechanism involved 42 species and 94 reversible chemical reactions (not counting the ranges of third-body collision efficiencies that were used). The reaction mechanism when N_2 dilution was considered involved 10 species and 19 reversible chemical reactions (not counting the ranges of third-body collision efficiencies that were used). Finally, the reaction mechanism when CO_2 dilution was considered involved 11 species and 19 reversible reactions (not counting the ranges of third-body collision efficiencies that were used). The backward rates for all mechanisms were found from chemical equilibrium requirements using the CHEMKIN package.[38]

Results and Discussion

Flame Stability and Evolution

Two kinds of flame instabilities were observed, as follows: 1) preferential-diffusion instability that was only observed when $Ma < 0$ and 2) hydrodynamic instability that was observed for all flame conditions. Buoyant instabilities observed during earlier work, for example, Kwon et al.,[8] were not observed during the present investigation due to the relatively large laminar flame speeds of the hydrogen-fueled flames that were considered. At conditions where $Ma < 0$, preferential-diffusion instability would eventually cause the flame surface to become wrinkled; however, flame surfaces remained smooth at small radii so that laminar burning velocities could still be measured for a time, even at these conditions. Thus, as noted earlier, no measurements were made at conditions where the flame surface was distorted or wrinkled due to effects of instabilities.

The presence of preferential-diffusion instability could be identified by the appearance of irregular (chaotic) wrinkling of the flame surface relatively early in the flame propagation process. Typical examples of stable and unstable flames with respect to preferential-diffusion instability are shown illustrated in Fig. 1 where the smooth and spontaneously wrinkled flame surfaces for stable and unstable preferential-diffusion conditions are clearly evident. (Note that the irregular luminous ignition disturbance of Fig. 1a has been blocked out to simplify interpretation.) Notably, the reactant conditions for these two flames were identical: stoichiometric combustion of hydrogen and air at NTP. Thus, the only difference between the two flames was that the flame without suppressant was nearly neutral ($Ma \approx 0$), whereas the flame containing Halon 1301 (2 vol%) as a suppressant exhibits unstable preferential-diffusion behavior ($Ma = -2.2$). When it is noted that wrinkled unstable flames have increased burning velocities compared to smooth flames having the same laminar burning velocities [because wrinkled flame surfaces have more surface area for reaction, (see Ref. 7)], the results of Fig. 1 clearly demonstrate a potentially undesirable effect of a flame suppressant with respect to fire safety.

Hydrodynamic instability could be identified readily by the development of a somewhat regular cellular disturbance pattern on the flame surface, rather late in the flame propagation process, similar to the observations of Groff.[39] Shadowgraph photographs of the flame surfaces when hydrodynamic instabilities are present for outwardly propagating spherical flames appear in Ref. 8 and references cited therein.

Flame Response to Stretch

Measurements at finite flame radii involve finite values of flame stretch so that the laminar burning velocity at the largest r_f observed, $S'_{L\infty}$, still differs from the fundamental unstretched laminar burning velocity of a plane flame, $S_{L\infty}$. Thus, values of $S_{L\infty}$ were found from Eq. (2) by plotting $S'_{L\infty}/S_L$ as a function of Karlovitz number similar to past work.[8–16] This yielded linear plots so that extrapolation to $Ka = 0$ gave $S'_{L\infty}/S_{L\infty}$ and, thus, $S_{L\infty}$, as summarized in Table 1. Then given $S_{L\infty}$, plots of $S_{L\infty}/S_L$ as a function

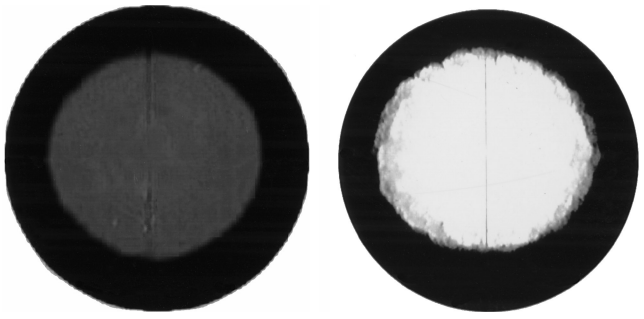

a) b)

Fig. 1 Flash shadowgraph photographs of stoichiometric H_2/air flames at NTP: a) without Halon 1301, which yields a near-neutral flame ($Ma \approx 0.0$) and b) with Halon 1301 (at a concentration of 2 vol%), which yields an unstable flame ($Ma = -2.2$).

of Kalovitz number can be constructed for various fuel equivalence ratios and concentrations of flame suppressants, also as suggested by Eq. (2). Examples of plots of this type for H_2/air flames at NTP, with $\phi = 0.6$, 1.0, and 1.8 and Halon 1301 concentrations of 0, 1, and 2 vol% are given in Fig. 2. Results at all other test conditions were qualitatively similar to Fig. 2.

The measurements shown in Fig. 2 illustrate the linear relationship between $S_{L\infty}/S_L$ and Karlovitz number that was exploited to find $S_{L\infty}$; similar linear behavior has been observed during all earlier experimental and computational studies of flame/stretch interactions of premixed flames in this laboratory.[8–16] The slope of these plots is equal to Markstein number according to Eq. (2), which is independent of Karlovitz number over the range of the measurements appearing in Fig. 2 (which involves $Ka < 0.15$). Similar behavior was observed over the entire range of the measurements (which involves $Ka < 0.75$), and the resulting constant values of Markstein number also are summarized in Table 1. Note, however, that quenching effects as extinction conditions are approached [where Karlovitz number would be on the order of unity (see Law[5])] would probably yield a more complex response to stretch. Even for the present range of Karlovitz number, however, effects of flame stretch are significant, for example, for the test conditions shown in Fig. 2, $S_{L\infty}/S_L$ varies in the range 0.6–1.2 for $Ka < 0.15$.

The measurements shown in Fig. 2 also exhibit interesting effects of fuel-equivalence ratio and concentration of Halon 1301 on flame stability to preferential-diffusion/stretch interactions. First, note that flames where increases of Karlovitz number cause $S_{L\infty}/S_L$ to decrease imply negative Markstein numbers from Eq. (2) and unstable preferential-diffusion behavior because the resulting increases of S_L with increasing Karlovitz number cause small disturbances of the flame surface to grow (see Refs. 8 and 9). In contrast, flames where increases of Karlovitz number cause $S_{L\infty}/S_L$ to increase imply positive Markstein numbers from Eq. (2) and stable preferential-diffusion behavior because resulting decreases of S_L with increasing Karlovitz number cause small disturbances to decay (see Refs. 8 and 9). To help distinguish these conditions in Fig. 2, unstable and stable conditions are denoted by closed and open symbols, respectively.

The general characteristic of unstable behavior ($Ma < 0$) at fuel-lean conditions and stable behavior ($Ma > 0$) at fuel-rich conditions, seen in Fig. 2, is consistent with conventional explanations of flame stability based on preferential diffusion of the deficient reactant proposed by Manton et al.[1]; also see Kwon et al.,[8] Aung et al.,[11] and references cited therein. Behavior at intermediate fuel-equivalence ratios (between $\phi \approx 1.0$ and 1.8) is more complex, however, and involves combined effects of preferential diffusion of both mass and heat.[16] Another interesting trend, however, is the progressive decrease of Markstein number toward more negative values as the concentration of the fire suppressant Halon 1301 is increased, a tendency that was observed at all fuel-equivalence ratios. In fact, for $\phi = 1.0$, this effect causes the nearly neutral flame in the absence of Halon 1301 to become decidedly unstable to preferential-diffusion effects at the maximum concentration of Halon 1301 considered during the present tests (2 vol%) as has already been illustrated and discussed in connection with Fig. 1. Unstable flame behavior causes increased rates of flame propagation for both laminar and turbulent premixed flames, due to the corresponding increase of overall reaction rate that results from the increase of flame surface area available for reaction.[7,8] This behavior clearly tends to counteract the ability of a flame suppressant, for example, Halon 1301, to reduce combustion rates by reducing laminar burning velocities, thus, tending to reduce its flame suppressing effectiveness to some extent.

Unstretched Laminar Burning Velocities

Measurements and predictions of $S_{L\infty}$ as a function of flame suppressant concentration are plotted in Fig. 3 for hydrogen/air flames

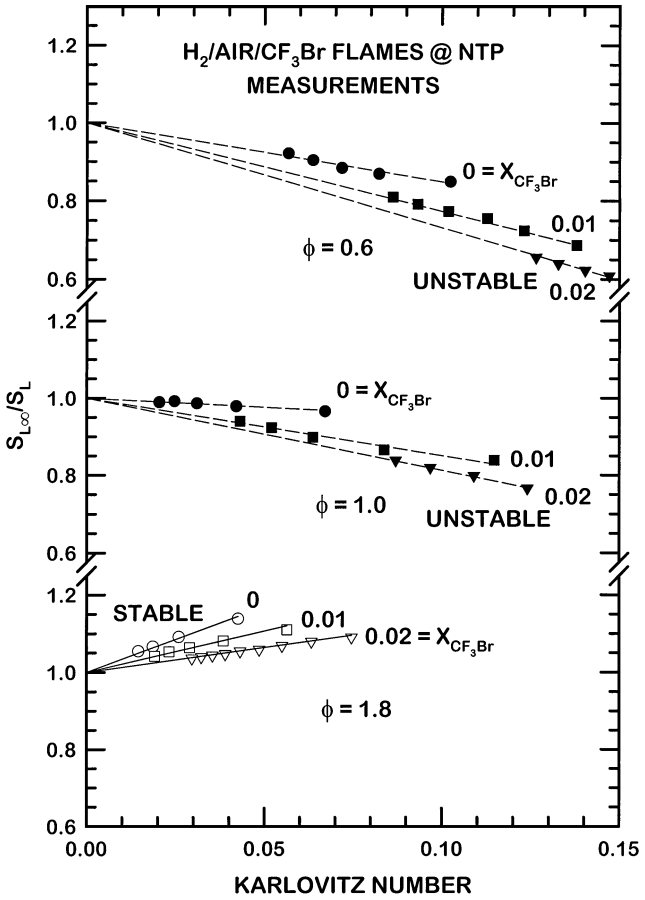

Fig. 2 Measured laminar burning velocities as a function of Karlovitz number, fuel-equivalence ratio, and concentration of Halon 1301 for H_2/air flames at NTP.

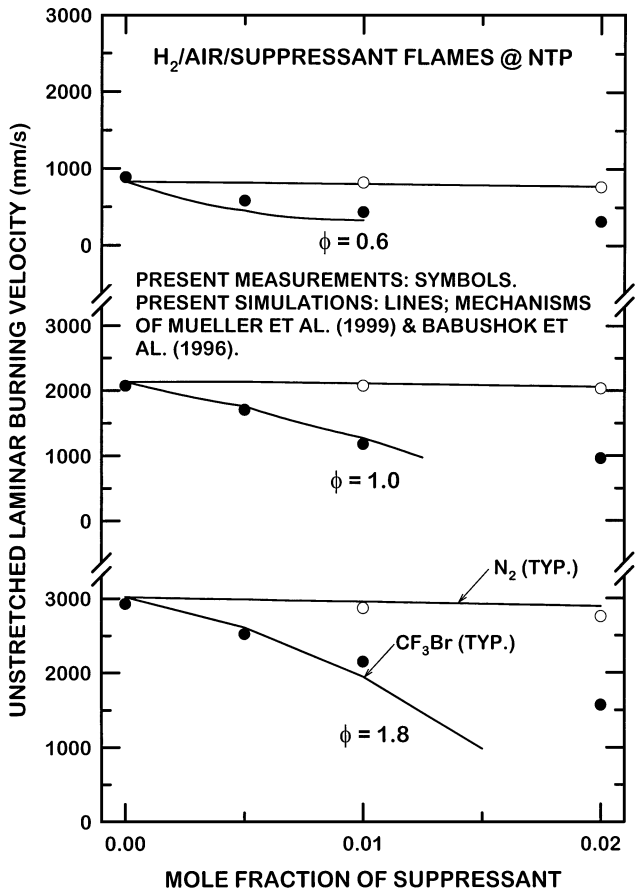

Fig. 3 Measured and predicted unstretched laminar burning velocities as a function of fuel-equivalence ratio and concentrations of Halon 1301 and nitrogen for H_2/air flames at NTP.

at NTP having fuel-equivalence ratios of 0.6, 1.0, and 1.8. Two types of flame suppressants are considered for the results shown in Fig. 3; namely, Halon 1301, which is a typical chemically active flame suppressant, and nitrogen, which is a typical chemically passive (chemically inert) or thermal-quenching type of flame suppressant.

The comparison between measured and predicted values of $S_{L\infty}$ in Fig. 3 is seen to be reasonably good. The satisfactory predictions of the laminar burning velocities of H/O reaction systems without Halon 1301 present follow from the good performance of flame property predictions for the Mueller et al.[37] kinetics for various types of passive diluents within H/O reactant mixtures that was observed by Kwon and Faeth.[16] Predictions of effects of Halon 1301 using the present simplification of the kinetics of Babushok et al.[21] were also reasonably satisfactory for modest concentrations of this suppressant, for example, concentrations less than 1 vol%. At larger concentrations of Halon 1301, however, this approach became problematical, and converged solutions for flame structure could no longer be obtained due to the unrealistically small laminar burning velocities obtained using the approximate mechanism at these conditions. This difficulty is felt to be due to the present simplified treatment of CF_3 chemistry that was used to treat effects of CF_3 that enters the reactant mixture as Halon 1301 is added to the system; however, more study of the Halon 1301 mechanism at large concentrations of this suppressant clearly is needed.

The results in Fig. 3 show that the chemically active suppressant Halon 1301 is much more effective as a suppressant than the chemically passive suppressant nitrogen, typical of numerous past studies of effects of Halon flame suppressants on the laminar burning velocities of laminar premixed flames involving a variety of reactants.[19–24] This behavior follows because nitrogen only acts to reduce laminar burning velocities by reducing chemical reaction rates in the flame as a result of flame temperature reductions due to dilution. Thus, flame temperature changes for the limited levels of dilution considered in Fig. 3 are rather small (summary shown in Table 1) so that the corresponding changes of laminar burning velocities really are not significant compared to experimental uncertainties. In contrast, the chemically active suppressant Halon 1301 causes a maximum reduction of $S_{L\infty}$ of nearly 70% for suppressant concentrations less than 1 vol% based on the predictions, and a maximum reduction of $S_{L\infty}$ of nearly 50% for suppressant concentrations less than 2% based on the measurements.

It is generally agreed that chemically active Halon flame suppressants reduce laminar burning velocities by acting to reduce concentrations of the H radical in the reaction zone of premixed flames.[19–24] This conclusion is supported by the close correlation between laminar burning velocities and H-radical concentrations pointed out by Padley and Sugden,[17] which was mentioned earlier and noted by many others.[16,19–24] The reduction of H-radical concentrations reduces the available radical pool and correspondingly lowers the rate of chain branching by the reaction $H + O_2 = OH + O$ with the corresponding reduction of the laminar burning velocity following from the reduced reaction rates.[19,20,24] The specific details of the way that Halon 1301 accomplishes the reduction of H-radical concentrations in the reaction zone of premixed laminar flames, however, are complex, and a variety of mechanisms can dominate the process, depending on the properties of the reactant mixture.[19–24] At a simple conceptual level, when it is noted that the C–Br bond is the weakest bond in the CF_3Br molecule and that, similar to CH_3, CF_3 is a relatively unreactive radical, CF_3Br can be thought of as a carrier of Br into the reaction zone, where it combines with hydrogen to form HBr. In turn, HBr becomes an inhibiting species through the following cycle of reactions described by Westbrook[19] (denoted cycle 1):

$$H + HBr = H_2 + Br, \qquad H + Br_2 = HBr + Br$$

$$Br + Br + M = Br_2 + M$$

where M stands for any molecule in the mixture. The net result of cycle 1 is the recombination of two H atoms into a relatively unreactive H_2 molecule, for example, $H + H = H_2$, which is catalyzed by the presence of HBr. On the other hand, Casias and McKinnon[24] show that, when concentrations of CF_3Br are small (less than roughly 4 vol% for the ethylene/air flames at NTP that they considered), cycle 1 is no longer the dominant suppression reaction path because the $Br + Br + M$ reaction becomes slow at these conditions and a catalytic cycle such as cycle 1 only proceeds as fast as its slowest step. Instead, they find four distinct reactions by which CF_3Br inhibits combustion, listed in their order of importance, as follows (denoted reaction series 2)[24]:

$$H + CF_3Br \rightarrow CF_3 + HBr, \qquad H + HBr \rightarrow H_2 + Br$$

$$CF_3Br \rightarrow CF_3 + Br, \qquad Br + HO_2 \rightarrow HBr + O_2$$

For reaction series 2, the first reaction involves H-atom trapping by CF_3Br in the preheat and reaction zones; the second reaction involves H-atom scavenging by HBr in the preheat and reaction zones; the third reaction involves endothermic dissociation of CF_3Br, which reduces temperatures (and thus reaction rates) in the reaction zone; and the fourth reaction involves free-radical termination in the preheat zone.[24] Present flames also involved small CF_3Br concentrations (less than 2 vol%) relevant to the reaction series 2 mechanism and yielded results generally consistent with the findings of Casius and McKinnon.[24] Finally, based on the findings of Noto et al.,[22] it is likely that subsequent decomposition of CF_3, and reaction of the resulting fragments, becomes important as CF_3Br concentrations increase; therefore, ignoring these reactions is mainly responsible for the present relatively poor prediction of effects of CF_3Br on $S_{L\infty}$ for concentrations of CF_3Br greater than 1 vol% in Fig. 3.

The effect of chemically passive flame suppressants on the unstretched laminar burning velocities of H_2/air flames is illustrated further by the results plotted in Fig. 4. These results include predictions and measurements of unstretched laminar burning velocities of stoichiometric H_2/air mixtures at NTP, considering N_2 and CO_2 for suppressant concentrations up to 50 vol%. The concentrations of suppressants are shown two ways in Fig. 4, as the mole fraction of the diluent and as the oxygen index. The latter parameter is a common measure of chemically passive flame suppressant performance[40]: It is defined as the concentration of oxygen in the suppressed reactant mixture in percent by volume. First, it is evident that present predictions are in good agreement with the measurements for the full range of conditions shown in Fig. 4. Next, the very much reduced effectiveness of the chemically passive (N_2 and CO_2) flame suppressants shown in Fig. 4, compared to the chemically active (CF_3Br) flame suppressant shown in Fig. 3, is quite evident. For example, concentrations of N_2 and CO_2 of 20–30 vol% are required to reduce $S_{L\infty}$ of stoichiometric H_2/air mixtures from the unsuppressed value of 2070 mm/s to roughly 1000 mm/s, whereas concentrations of CF_3Br of only 1 vol% are required for the same reduction. Finally, CO_2 is seen to be slightly more effective for reducing $S_{L\infty}$ than

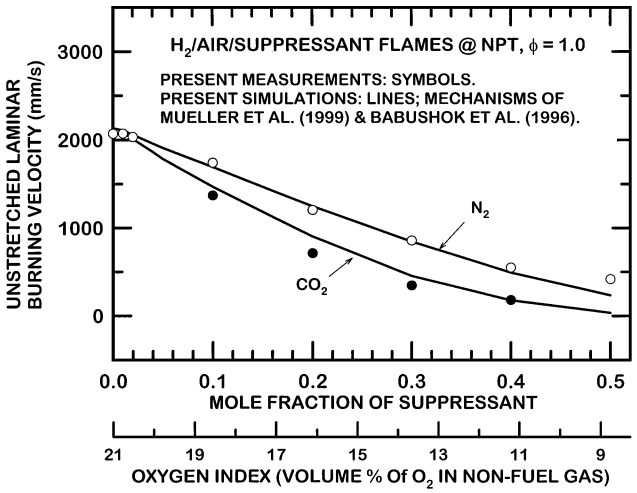

Fig. 4 Measured and predicted unstretched laminar burning velocities as a function of concentrations of nitrogen and carbon dioxide for stoichiometric H_2/air flames at NTP.

N_2. This behavior is expected, however, because the specific heat of the triatomic molecule CO_2 is greater than that of the diatomic molecule N_2. As a result, similar concentrations of these two flame suppressants imply smaller flame temperatures for the flames suppressed with CO_2 than with N_2. For example, the addition of 40 vol% of flame suppressant reduces flame temperatures from the unsuppressed value of 2380 to 1230 K for CO_2 but only to 1680 K for N_2 for the conditions of Fig. 4 (see Table 1). The corresponding reduced reaction rates in the flame zone of the CO_2-suppressed flame compared to the N_2-suppressed flame then implies smaller values of $S_{L\infty}$ as well.[41,42]

Markstein Numbers

As discussed earlier, Markstein numbers are independent of Karlovitz numbers for present conditions and are summarized in Table 1 as a function of reactant conditions. Measured Markstein numbers for H_2/air flames at $\phi = 0.6$, 1.0, and 1.8 are plotted as a function of the suppressant concentration in Fig. 5, considering results for both Halon 1301 and nitrogen as suppressants. Similar to earlier findings,[16] values of the Markstein number become progressively more negative as ϕ decreases, so that preferential-diffusion instability is promoted as the flames become leaner. This behavior satisfies classical models of flame instability due to effects of preferential diffusion,[1,2] namely, that laminar premixed flames are unstable to effects of preferential-diffusion at conditions where the fast diffusing component (H_2 in the present instance) is deficient (at lean conditions in the present instance). In addition, increased concentrations of both suppressants cause the Markstein number to decrease most dramatically for Halon 1301, tending to enhance potential effects of preferential-diffusion instability at all three fuel-equivalence ratios shown in Fig. 5. As already discussed in connection with Fig. 1, results at $\phi = 1$ are particularly interesting in this regard because these flames exhibit near-neutral stability ($Ma \approx 0$) when no suppressant is present but exhibit significant degrees of preferential-diffusion instability as concentrations of Halon 1301 increase toward 2 vol% (where $Ma \rightarrow -2.2$). In addition, the results shown in Fig. 1 demonstrate that this transition is properly reflected by a smooth flame surface when $Ma \approx 0$ and a chaotically disturbed flame surface due to preferential-diffusion instability when $Ma \rightarrow -2.2$. Finally, the results summarized in Table 1 show that increased amounts of both chemically active and chemically passive suppressants generally cause Markstein numbers to become progressively more negative.

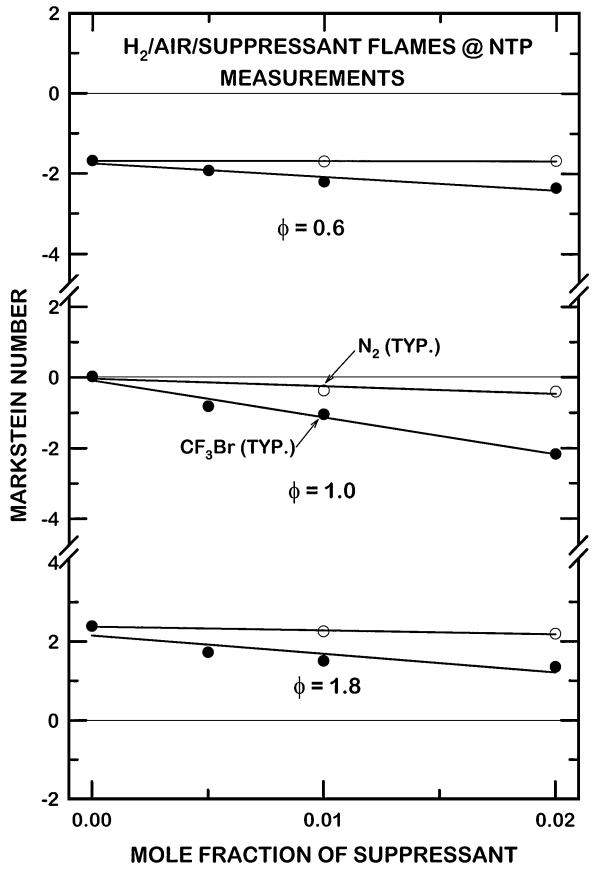

Fig. 5 Measured Markstein numbers as a function of fuel-equivalence ratio and the concentrations of Halon 1301 and nitrogen for H_2/air flames at NTP.

Flame Structure

As mentioned earlier, measurements and predictions of $S_{L\infty}$ were in reasonably good agreement, including effects of flame suppressants; therefore, the predictions were exploited to gain a better understanding of effects of flame suppressants on laminar burning velocities. The approach involved numerical simulations of plane H_2/air flames for various fuel-equivalence ratios and suppressant concentrations, considering Halon 1301, nitrogen, and carbon dioxide as suppressants.

Typical predicted structures of H_2/air flames at NTP, with and without Halon 1301 suppressant present, are shown in Figs. 6 and 7 (based on the kinetics of Mueller et al.[37] and Babushok et al.[21]). Temperatures and stable species concentrations are plotted in Fig. 6, whereas radical species concentrations are plotted in Fig. 7. The conditions illustrated involve stoichiometric reactant mixtures with Halon 1301 concentrations of 0 and 1 vol%. (Recall that these two

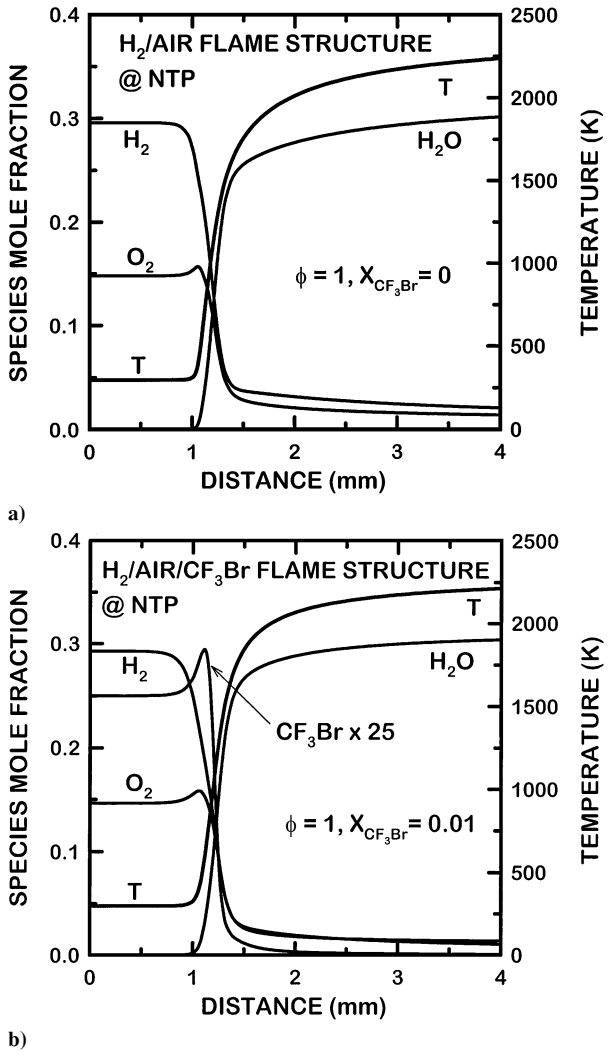

Fig. 6 Predicted temperature and major species structure of stoichiometric H_2/air flames at NTP: a) without Halon 1301, which implies a near-neutral flame ($Ma \approx 0.0$) and b) with Halon 1301 at a concentration of 1 vol%, which implies an unstable flame ($Ma = -1.1$).

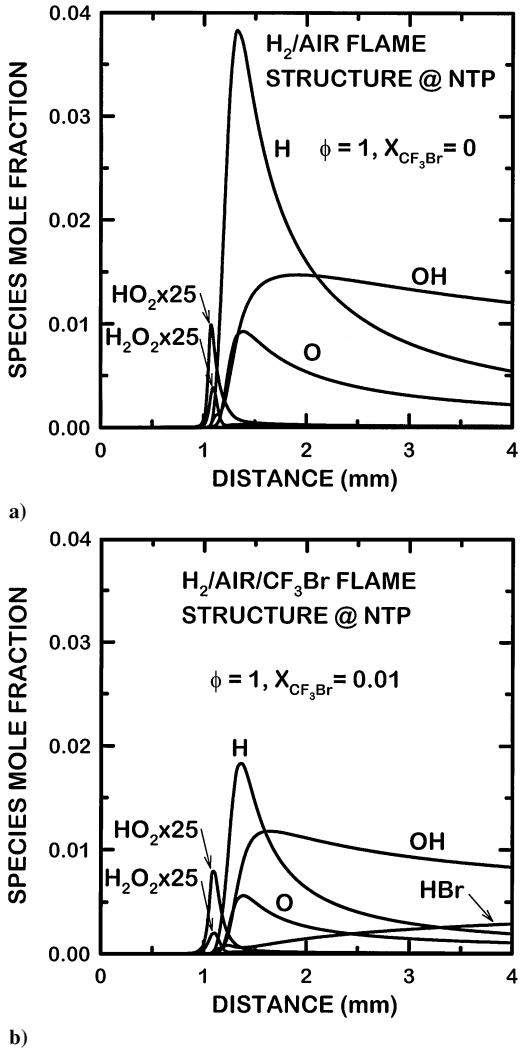

Fig. 7 Predicted radical structure of stoichiometric H_2/air flames at NTP: a) without Halon 1301, which implies a near-neutral flame ($Ma \approx 0.0$) and b) with Halon 1301 at a concentration of 1 vol%, which implies an unstable flame ($Ma = -1.1$).

conditions represent near-neutral and unstable preferential-diffusion conditions, respectively, with corresponding smooth and wrinkled flame surfaces similar to those appearing in Fig. 1.) Results in Figs. 6 and 7 include distributions of temperatures and species mole fractions as a function of distance through the flames. The origins of the length scales for both flames are arbitrary. The concentrations of CF_3Br are much smaller than other stable species in the suppressant-containing flame and have been multiplied by a factor of 25 so that its concentration distribution can be seen. Finally, the results show that the maximum concentrations of the radicals HO_2 and H_2O_2 are roughly two orders of magnitude smaller than those of H, OH and O; therefore, these concentrations are also multiplied by a factor of 25 so that their concentration distributions can be seen.

When the results for temperature and stable species concentrations in Fig. 6 are considered, it is evident that the addition of the flame suppressant has very little effect on flame temperatures because the degree of dilution of the flame by the present limited amounts of suppressant used is small, as noted in connection with Table 1. Effects of preferential diffusion of mass are important in these flames, however, as can be seen from the concentration distributions of O_2 and CF_3Br appearing in Fig. 6. In particular, mass diffusivities decrease in the order $H_2 > O_2 > CF_3Br$ so that the more rapid transport of H_2 compared to O_2 toward the reaction zone of the flame without the flame suppressant causes a peak to appear in the concentration distribution of O_2 near the cold boundary of the flame. The O_2 peak also appears in the flame with the flame suppressant present, but in addition, a somewhat larger peak appears in the concentration distribution of CF_3Br near the cold boundary of the flame because it is transported at the slowest rate of all of the stable species in this flame. Reaction of CF_3Br causes this suppressant to eventually disappear in the reaction zone, similar to the other reactants for the present stoichiometric flame conditions. Effects of preferential diffusion of heat and mass in these flames are also present as discussed by Kwon and Faeth,[16] although these effects are not easily distinguished based on the results shown in Fig. 6.

The results for the concentrations of radical species in flames with and without suppressants shown in Fig. 7 show immediately the dramatic reduction of radical concentrations in the reaction zone due to the presence of the flame suppressant, even for the present small concentrations of CF_3Br added to the flame, for example, the addition of CF_3Br of 1 vol% causes concentrations of H and most other radicals to decrease by roughly 50%. Based on the findings of Kwon and Faeth[16] for flames having hydrogen and oxygen as reactants, it would be expected that the reduced radical pool of the CF_3Br-containing flame would tend to promote preferential-diffusion instability, for example, to reduce the value of the Markstein number of the CF_3Br-containing flame compared to the flame having no suppressant.

Radical Behavior

The flame structure results of Fig. 7, and similar results presented earlier by Kwon and Faeth,[16] indicate that the H radical has the highest concentrations of all of the radicals in flames having hydrogen and oxygen as reactants, even for lean flames having fuel-equivalence ratios as small as $\phi = 0.6$, which was the smallest value of ϕ considered during these two investigations. In addition, OH-radical concentrations are comparable to H-radical concentrations within fuel-lean flames of these reactants. This behavior is significant due to the strong correlation between laminar burning velocities and H-radical concentrations in the flame reaction zone.[16,17,42] Thus, it was of interest to see whether this correlation would continue when the radical pool in the flame reaction zone was affected by a flame suppressant.

Similar to past work, the most robust correlation between laminar burning velocities and radical concentrations for flames having hydrogen and oxygen as reactants was obtained by considering the sum of the mole fractions of H and OH at the position where the mole fraction of the H radical was a maximum in the flame. The resulting correlation is shown in Fig. 8, where the value of S_L is

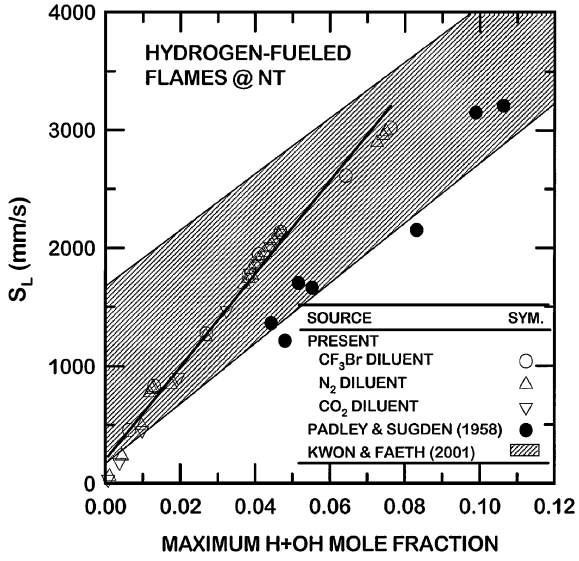

Fig. 8 Measured and computed laminar burning velocities as a function of maximum H + OH mole fractions in the reaction zone of hydrogen/air flames with and without Halon 1301. Results from Padley and Sugden[17] and Kwon and Faeth[16] without Halon 1301; results from the present investigation with Halon 1301.

plotted as a function of the maximum values of the mole fractions of H and OH found as just described. Results (for normal temperature) shown in Fig. 8 include findings from Padley and Sugden,[17] Kwon and Faeth,[16] and the present investigation. The results from Padley and Sugden[17] were obtained by direct measurements of radical concentrations in the flames combined with the laminar burning velocity measurements of Jahn (cited in Ref. 18); unfortunately, these results involve effects of unknown levels of flame stretch. [The findings of Aung et al.[10] suggest that S_L values are roughly 10% lower than the unstretched values of S_L for the results of Jahn (see Ref. 18), but the corresponding effects of stretch on the radical concentrations measured by Padley and Sugden[17] are unknown.] The results of Kwon and Faeth[16] were obtained considering outwardly propagating spherical flames with values of S_L found using the present methods for both stretched and unstretched laminar premixed flames (with flame structure found for stretched flames using the RUN-1DL algorithm of Rogg[43]). The results of Kwon and Faeth[16] use a normalized unstretched laminar burning velocity to account for effects of pressure; however, this approach has not been used for the other results in Fig. 1, which are limited to atmospheric pressure. Finally, the present results involved the same experimental methods as Kwon and Faeth[16] to find S_L and $S_{L\infty}$. Similarly, the present flame structures were found using the same chemical kinetics and thermodynamic and transport properties as Kwon and Faeth,[16] but present flame structure computations used the PREMIX algorithm of Kee et al.,[33] whereas Kwon and Faeth[16] used the RUN1-DL algorithm of Rogg.[43] In addition, the present results involve effects of both chemically active (CF_3Br) and chemically passive (N_2 and CO_2) flame suppressants. Clearly, there is a rough correlation between the laminar burning velocities and the maximum concentrations of H + OH, with the concentrations of these radicals varied in a variety of ways: various diluent concentrations, various fuel-equivalence ratios, various degrees of flame stretch, various concentrations of a chemically active flame suppressant (CF_3Br), and various concentrations of chemically passive flame suppressants (N_2 and CO_2). This behavior supports the widely held hypothesis that the effect of flame suppressants on the laminar burning velocities of flames involving hydrogen and oxygen as reactants can largely be attributed to the capability of these materials to reduce H-radical concentrations in the reaction zone and, thus, overall concentrations of the radical pool within the reaction zone by affecting the chain branching reaction $H + O_2 = OH + O$ (as can be seen from Fig. 7).

Conclusions

Effects of flame stretch and the concentrations and types of flame suppressants on the laminar burning velocities of hydrogen/air reactant mixtures at NTP were studied both experimentally and computationally. The experiments involved outwardly propagating laminar spherical flames similar to past work in this laboratory[8–16]; the computations were limited to fundamental (unstretched) flames considering the detailed reaction mechanisms of Mueller et al.[37] for H_2/O_2 chemistry and Babushok et al.[21] for Halon chemistry using the PREMIX algorithm of Kee et al.[33] The reactant mixtures were at NTP with fuel-equivalence ratios of 0.6–1.8, with Halon 1301 as a chemically active flame suppressant having concentrations up to 2 vol%, and with N_2 and CO_2 as chemically passive flame suppressants having concentrations up to 50 vol%. Karlovitz numbers in the range 0–0.15 yielded ratios of unstretched/stretched laminar burning velocities of 0.6–1.2. The major conclusions of the study are as follows:

1) Effects of flame/stretch interactions for the measurements of suppressed flames could be correlated based on the local-conditions hypothesis according to $S_{L\infty}/S_L = 1 + Ma\,Ka$ to obtain a linear relationship between $S_{L\infty}/S_L$ and Karlovitz number, yielding constant Markstein numbers for given reactant conditions, similar to earlier findings for unsuppressed flames.

2) Effects of flame stretch on laminar burning velocities were substantial, yielding values of $S_{L\infty}/S_L$ in the range 0.6–1.2, even though present flames did not approach quenching conditions; corresponding Markstein numbers were in the range −2.4–2.5.

3) Predicted and measured unstretched laminar burning velocities for the chemically active suppressant Halon 1301 were in reasonably good agreement using the H_2/O_2 reaction mechanism of Mueller et al.[37] and the Halon reaction mechanism of Babushok et al.[21]; nevertheless, there were discrepancies between measured and predicted effects of Halon 1301 for concentrations greater than 1 vol%, probably due to the present simplified treatment of the reaction properties of CF_3. Corresponding predictions of unstretched laminar burning velocities for the chemically passive suppressants, N_2 and CO_2, were reasonably satisfactory for suppressant concentrations up to 50 vol%, the largest concentrations considered during this investigation.

4) Present predictions of flame structure support past observations that the strong flame suppression capabilities of Halon 1301 are due to its ability to reduce concentrations of radicals in the radical pool of the reaction zone of flames involving H_2 and O_2 as reactants. In addition, this capability appears to be due to CF_3Br participating in the four distinct reactions of reaction series 2 as suggested by Casias and McKinnon[24] for flames suppressed by relatively small concentrations of CF_3Br (less than 2 vol% for present experiments).

5) Predictions showed that the laminar burning velocities of the present H_2/air flames were strongly correlated with the maximum H + OH-radical concentrations in the reaction zone for variations of these concentrations due to effects of flame suppressants, similar to an early proposal of Padley and Sugden[17] for unsuppressed and unstretched hydrogen/air flames and recent observations of Kwon and Faeth[16] for a variety of unsuppressed and stretched and unstretched flames having H_2 and O_2 as reactants.

6) Present findings suggest that H and OH radical production and transport are important aspects of preferential-diffusion/stretch interactions in flames involving H_2 and O_2 as reactants and that conditions that reduce the concentrations of these radicals in the reaction zone tend to enhance unstable preferential-diffusion effects in these flames. Thus, the very tendency of flame suppressants to reduce laminar burning velocities (and, thus, tend to reduce fire hazards) by reducing radical concentrations in the reaction zone of flames also gives rise to increased flame surface areas and correspondingly increased flame reaction rates due to the presence of preferential-diffusion instabilities that are promoted by the reduced radical concentrations in the reaction zone of flames (and thus tend to increase fire hazards).

Finally, practical fires involve both premixed and nonpremixed flame effects, whereas present findings are limited to premixed flames; clearly, the results of similar considerations for nonpremixed flames are needed.

Acknowledgments

This research was supported in part by National Science Foundation Grant 9321959 under the technical management of F. Fisher. Support from the Rackham Fellowship Program of the University of Michigan for O. C. Kwon is also gratefully acknowledged.

References

[1]Manton, J., von Elbe, G., and Lewis, B., "Nonisotropic Propagation of Combustion Waves in Explosive Gas Mixtures and Development of Cellular Flames," *Journal of Chemical Physics*, Vol. 20, No. 1, 1952, pp. 153–158.

[2]Markstein, G. H., *Non-Steady Flame Propagation*, Pergamon, New York, 1964, p. 22.

[3]Strehlow, R. A., and Savage, L. D., "The Concept of Flame Stretch," *Combustion and Flame*, Vol. 31, No. 2, 1978, pp. 209–211.

[4]Clavin, P., "Dynamic Behavior of Premixed Flame Fronts in Laminar and Turbulent Flows," *Progress in Energy and Combustion Science*, Vol. 11, No. 1, 1985, pp. 1–59.

[5]Law, C. K., "Dynamics of Stretched Flames," *Proceedings of the Combustion Institute*, Vol. 22, 1988, pp. 1381–1402.

[6]Vagelopoulos, C. M., Egolfopoulos, F. N., and Law, C. K., "Further Considerations on the Determination of Laminar Flame Speeds with the Counterflow Twin-Flame Technique," *Proceedings of the Combustic Institute*, Vol. 25, 1994, pp. 1341–1347.

[7]Aung, K. T., Hassan, M. I., Kwon, O. C., Tseng, L.-K., and Faeth, G. M., "Flame/Stretch Interactions in Laminar and Turbulent Premixed Flames," *Combustion Science and Technology*, Vol. 173, No. 1, 2002, pp. 61–99.

[8]Kwon, S., Tseng, L.-K., and Faeth, G. M., "Laminar Burning Velocities and Transition to Unstable Flames in $H_2/O_2/N_2$ and $C_3H_8/O_2/N_2$ Mixtures," *Combustion and Flame*, Vol. 90, No. 3, 1992, pp. 230–246.

[9]Tseng, L.-K., Ismail, M. A., and Faeth, G. M., "Laminar Burning Velocities and Markstein Numbers of Hydrocarbon/Air Flames," *Combustion and Flame*, Vol. 95, No. 4, 1993, pp. 410–426.

[10]Aung, K. T., Hassan, M. I., and Faeth, G. M., "Flame/Stretch Interactions of Laminar Premixed Hydrogen/Air Flames at Normal Temperature and Pressure," *Combustion and Flame*, Vol. 109, No. 1/2, 1997, pp. 1–24.

[11]Aung, K. T., Hassan, M. I., and Faeth, G. M., "Effects of Pressure and Nitrogen Dilution on Flame/Stretch Interactions of Laminar Premixed $H_2/O_2/N_2$ Flames," *Combustion and Flame*, Vol. 112, No. 1/2, 1998, pp. 1–15.

[12]Hassan, M. I., Aung, K. T., and Faeth, G. M., "Properties of Laminar Premixed CO/H_2/Air Flames at Various Pressures," *Journal of Propulsion and Power*, Vol. 13, No. 2, 1997, pp. 239–245.

[13]Hassan, M. I., Aung, K. T., Kwon, O. C., and Faeth, G. M., "Properties of Laminar Premixed Hydrocarbon/Air Flames at Various Pressures," *Journal of Propulsion and Power*, Vol. 14, No. 4, 1998, pp. 479–488.

[14]Hassan, M. I., Aung, K. T., Kwon, O. C., and Faeth, G. M., "Measured and Predicted Properties of Laminar Premixed Methane/Air Flames at Various Pressures," *Combustion and Flame*, Vol. 115, No. 4, 1998, pp. 539–550.

[15]Kwon, O. C., Hassan, M. I., and Faeth, G. M., "Flame/Stretch Interactions of Premixed Fuel-Vapor/O_2/N_2 Flames," *Journal of Propulsion and Power*, Vol. 16, No. 3, 2000, pp. 513–522.

[16]Kwon, O. C., and Faeth, G. M., "Flame/Stretch Interactions of Premixed Hydrogen-Fueled Flames: Measurements and Predictions," *Combustion and Flame*, Vol. 124, No. 4, 2001, pp. 590–610.

[17]Padley, P. J., and Sugden, T. M., "Chemiluminescence and Radical Recombination in Hydrogen Flames," *Proceedings of the Combustion Institute*, Vol. 7, 1958, pp. 235–244.

[18]Lewis, B., and von Elbe, G., *Combustion Flames and Explosions of Gases*, 3rd ed., Academic Press, New York, 1987, pp. 395–402.

[19]Westbrook, C. K., "Inhibition of Hydrocarbon Oxidation in Laminar Flames and Detonations by Halogenated Compounds," *Proceedings of the Combustion Institute*, Vol. 19, 1982, pp. 127–141.

[20]Westbrook, C. K., "Numerical Modeling of Flame Inhibition of CF_3 Br," *Combustion Science and Technology*, Vol. 34, No. 1–6, 1983, pp. 201–225.

[21]Babushok, V., Noto, T., Burgess, D. R., Jr., Hamins, A., and Tsang, W., "Influence of CF_3I, CF_3Br, and CF_3H on the High-Temperature Combustion of Methane," *Combustion and Flame*, Vol. 107, No. 4, 1996, pp. 351–367.

[22]Noto, T., Babushok, V., Burgess, D. R., Jr., Hamins, A., Tsang, W., and Miziolek, A., "Effect of Halogenated Flame Inhibitors on C_1-C_2 Organic Flames,"*Proceedings of the Combustion Institute*, Vol. 26, 1996, pp. 1377–1383.

[23]Noto, T., Babushok, V., Hamins, A., and Tsang, W., "Inhibition Effectiveness of Halogenated Compounds," *Combustion and Flame*, Vol. 112, No. 1/2, 1998, pp. 147–160.

[24]Casias, C. R., and McKinnon, J. T., "A Modeling Study of the Mechanisms of Flame Inhibition by CF_3Br Fire Suppression Agent," *Proceedings of the Combustion Institute*, Vol. 27, 1998, pp. 2731–2739.

[25]McBride, B. J., Reno, M. A., and Gordon, S., "CET93 and CETPC: An Interim Updated Version of the NASA Lewis Computer Program for Calculating Complex Chemical Equilibrium with Applications," NASA TM 4557, 1994.

[26]Reynolds, W. C., "The Element Potential Method for Chemical Equilibrium Analysis: Implementation in the Interactive Program STANJAN," Dept. of Mechanical Engineering Rept., Stanford Univ., Stanford, CA, Jan. 1986.

[27]Kwon, O. C., "A Theoretical and Experimental Study of Preferential-Diffusion/Stretch Interactions of Laminar Premixed Flames," Ph.D. Dissertation, Aerospace Engineering, Univ. of Michigan, Ann Arbor, MI, May 2000.

[28]Taylor, S. C., "Burning Velocity and Influence of Flame Stretch," Ph.D. Dissertation, Mechanical Engineering, Univ. of Leeds, Leeds, England, U.K., Sept. 1991.

[29]Dowdy, D. R., Smith, D. B., Taylor, S. C., and Williams, A., "The Use of Expanding Spherical Flames to Determine Burning Velocities and Stretch Effects on Hydrogen/Air Mixtures," *Proceedings of the Combustion Institute*, Vol. 23, 1990, pp. 325–333.

[30]Brown, M. J., McLean, I. C., Smith, D. B., and Taylor, S. C., "Markstein Lengths of CO/H_2/Air Flames, Using Expanding Spherical Flames," *Proceedings of the Combustion Institute*, Vol. 26, 1996, pp. 875–882.

[31]Karpov, V. F., Lipatnikov, A. N., and Wolanski, P., "Finding the Markstein Number Using the Measurements of Expanding Spherical Laminar Flames," *Combustion and Flame*, Vol. 109, No. 3, 1996, pp. 436–448.

[32]Bradley, D., Hicks, R. A., Lawes, M., Sheppard, C. G. W., and Woolley, R., "The Measurements of Laminar Burning Velocities and Markstein Numbers for Iso-Octane-Air and Iso-Octane-n-Heptane in Air Mixtures at Elevated Temperatures and Pressures in an Explosion Bomb," *Combustion and Flame*, Vol. 115, No. 1/2, 1998, pp. 126–144.

[33]Kee, R. J., Grcar, J. F., Smooke, M. D., and Miller, J. A., "A FORTRAN Program for Modeling Steady Laminar One-Dimensional Premixed Flames," Rept. SAND85-8240, Sandia National Labs., Albuquerque, NM, Jan. 1993.

[34]Kee, R. J., Rupley, F. M., and Miller, J. A., "The CHEMKIN Thermodynamic Data Base," Rept. SAND87-8215B, Sandia National Labs., Albuquerque, NM, Oct. 1992.

[35]Kee, R. J., Dixon-Lewis, G., Warnatz, J., Coltrin, M. E., and Miller, J. A., "A FORTRAN Computer Code Package for the Evaluation of Gas-Phase, Multicomponent Transport Properties," Rept. SAND86-8246, Sandia National Labs., Albuquerque, NM, July 1992.

[36]Kim, T. J., Yetter, R. A., and Dryer, F. L., "New Results on Moist CO Oxidation: High Pressure, High Temperature Experiments and Comprehensive Modeling," *Proceedings of the Combustion Institute*, Vol. 25, 1994, pp. 759–766.

[37]Mueller, M. A., Kim, T. J., Yetter, R. A., and Dryer, F. L., "Flow Reactor Studies and Kinetic Modeling of the H_2/O_2 Reaction," *International Journal of Chemical Kinetics*, Vol. 31, No. 2, 1999, pp. 113–125.

[38]Kee, R. J., Rupley, F. M., and Miller, J. A., "CHEMKIN II: A FORTRAN Chemical Kinetics Package for the Analysis of Gas Phase Chemical Kinetics," Rept. SAND89-8009B, Sandia National Labs., Albuquerque, NM, Jan. 1993.

[39]Groff, E. G., "The Cellular Nature of Confined Spherical Propane-Air Flames," *Combustion and Flame*, Vol. 48, No. 1, 1982, pp. 51–62.

[40]Tuhtar, D., *Fire and Explosion Protection: A System Approach*, Wiley, New York, 1989, pp. 127–129.

[41]Huggett, C., "Combustion Processes in the Aerospace Environment," *Aerospace Medicine*, Vol. 40, 1969, pp. 1176–1180.

[42]Huggett, C., "Habitable Atmospheres Which do not Support Combustion," *Combustion and Flame*, Vol. 20, No. 1, 1973, pp. 140–142.

[43]Rogg, B., "RUN-1DL: The Cambridge Universal Laminar Flame Code," Dept. of Engineering, TR CUED/A-THERMO/TR39, Univ. of Cambridge, Cambridge, England, U.K., 1991.